  Bull. Chem. Soc. Jpn., 62, 2245—2251 (1989)

Structure and Optical Properties of a Thermochromic Schiff Base. Low-Temperature Structural Studies of the *N,N'*-Disalicylidene-*p*-phenylenediamine and *N,N'*-Disalicylidene-1,6-pyrenediamine Crystals

Tamotsu INABE,* Naomi HOSHINO,† Tadaoki MITANI, and Yusei MARUYAMA*
Institute for Molecular Science, Myodaiji, Okazaki 444
(Received October 24, 1988)

The crystal structure of *N,N'*-disalicylidene-*p*-phenylenediamine (BSP[1]) has been determined at 108 K. This compound shows a thermochromic-type behavior in the crystalline state; this chromism has been interpreted in terms of an intramolecular proton transfer from the hydroxyl oxygen to the imine nitrogen through the O-H···N hydrogen bond. In comparison with the room-temperature structure, no significant differences in the molecular structure and the molecular packing in the lattice have been observed. The room-temperature and low-termperature structures of another *N*-salicylideneaniline derivative, *N,N'*-disalicylidene-1,6-pyrenediamine (DSPY), have also been determined. In contrast to BSP, the absence of a thermal proton-transfer process in DSPY is suggested by optical measurements. Comparative studies of these two compounds indicate that a conjugation system which is not included in a π-electron configurational change by the proton transfer must be coplanar with the hydrogen-bonded chelate ring for the thermal proton transfer.

The room-temperature structure and optical properties of a thermochromic derivative of *N*-salicylideneaniline, BSP, have been reported recently.[2] The thermochromism of *N*-salicylideneanilines in the crystalline state was established to be due to the self-isomerization of a molecule by proton transfer from the hydroxyl oxygen to the imine nitrogen.[3] The temperature dependences of the visible absorption and emission spectra of BSP are consistent with this interpretation. The OH and/or NH vibrational modes in the infrared spectra are supposed to be sensitive to such an isomerization process. The OH stretching mode actually showed a significant change in the peak profile with varying the temperature.[2] However, the change has not completely been interpreted due to its complicated feature.

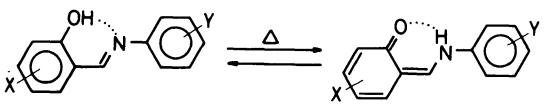

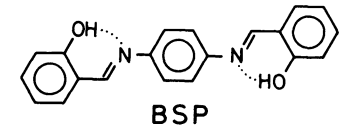

BSP

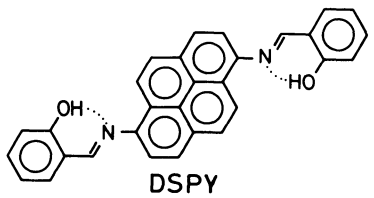

DSPY

Among the other *N*-salicylideneaniline derivatives, DSPY has been found to show no thermochromic behavior, although it has a similar framework to BSP. Thus, a comparison of BSP and DSPY is expected to provide some information about the conditions of the structure and the electronic state required for the proton transfer in *N*-salicylideneanilines. In order to make a clear comparison, it is desirable to employ the structures determined at low temperatures, since the temperature influences not only the thermal motion of atoms but also the thermochromic effects in the case of BSP. In this paper, the room-temperature structure and the optical properties of DSPY as well as the low-temperature structure and that of BSP are presented.

Experimental

Materials. DSPY was prepared by condensation of 1,6-pyrenediamine and salicylaldehyde in the same manner as BSP,[2] and was recrystallized from benzene. 1,6-Pyrenediamine was synthesized following the method reported by Vollman et al.[5]

Optical Measurements. Single-crystal measurements (infrared absorption and visible absorption and emission spectra) were performed by the same methods reported before.[2]

X-Ray Structure Analyses. An automated RIGAKU AFC-5R diffractometer with graphite monochromatized Mo $K\alpha$ radiation was used for data collection of DSPY at room temperature. Thirty-one reflections with $20°<2\theta<30°$ were used to determine the lattice parameters. The crystal data are listed in Table 1. The intensity data were collected in the region $2\theta>50°$ ($-25\leqq h\leqq 25$, $-15\leqq k\leqq 15$, $0\leqq l\leqq 4$) in the θ-2θ mode (scan width, $(1.2+0.5\tan\theta)°$) at a scan rate of 6° min^{-1}. Background counts at each end were 4—10.5 s. The intensities of the three standards, monitored every 100 data measurements, showed no significant variation. 4360 unique reflections were measured. After reducing the symmetry, 851 independent reflections with $|F_o|>3\sigma(F_o)$ were used for a structure analysis.

† Present address: Department of Chemistry, Faculty of Science, Hokkaido University, Sapporo 060.

Table 1. Crystal Data

	BSP (108 K)	DSPY (R.T.)	DSPY (108 K)
Chemical formula	$C_{20}H_{16}N_2O_2$	$C_{30}N_{20}N_2O_2$	$C_{30}N_{20}N_2O_2$
Molecular weight	316.35	440.49	440.49
Crystal color	Light yellow	Orange	Orange
Crystal size/mm	0.55×0.25×0.08	0.45×0.13×0.08	0.45×0.13×0.08
Crystal system	Monoclinic	Monoclinic	Monoclinic
Space group	$P2_1/c$	$P2_1/a$	$P2_1/a$
a/Å	14.605(4)	12.902(3)	12.837(3)
b/Å	4.551(1)	21.326(6)	21.396(7)
c/Å	12.092(4)	3.874(1)	3.795(1)
β/deg	112.87(2)	95.79(2)	95.53(3)
V/Å^3	740.5(4)	1060.6(5)	1037.4(5)
Z	2	2	2
D_c/g cm^{-3}	1.419	1.380	1.411
μ(Mo $K\alpha$)/cm^{-1}	0.867	0.811	0.830
R	0.048	0.046	0.047
R_w	0.059	0.050	0.048

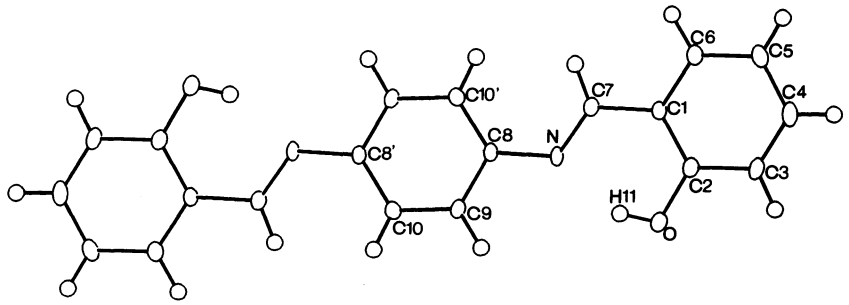

Fig. 1. ORTEP drawing[9] of BSP at 108 K showing the atom numbering scheme.

An automated RIGAKU AFC-5 diffractometer with a cold nitrogen gas flow equipment was used for the low-temperature data collection of BSP and DSPY. Twenty-five reflections for BSP and twenty-one reflections for BSDAP with $20°<2\theta<30°$ were used to determine the lattice parameters. The crystal data are shown in Table 1. The intensity data were collected in the region $2\theta<60°$ for both compounds ($-20\leqq h\leqq 18$, $0\leqq k\leqq 6$, $0\leqq l\leqq 17$ for BSP; $-17\leqq h\leqq 17$, $0\leqq k\leqq 30$, $0\leqq l\leqq 5$ for DSPY) in θ-2θ mode (scan width, $(1.2+0.5\tan\theta)°$) at a scan rate of 3° min^{-1}. Background counts at each end were 8—21.5 s. The intensities of the three standards, monitored every 100 data measurements, remained constant within 1% for both compounds. 2525 unique reflections for BSP and 3529 unique reflections for DSPY were measured. 1050 independent reflections (BSP) and 1160 reflections (DSPY) with $|F_o|>3\sigma(F_o)$ were used for structure analyses.

Crystal structures were solved by a direct method and all hydrogen atoms were determined from difference synthesis maps. A block-diagonal least-squares technique (UNICS III[6]) with anisotropic thermal parameters for nonhydrogen atoms and isotropic for hydrogen atoms (weighting scheme, $1/w=\sigma^2+(0.015|F_o|)^2$) was employed for the structure refinement.

Results and Discussion

BSP. The molecular structure derived at 108 K is shown in Fig. 1; the atomic parameters are listed in Table 2.[7] As can be seen from the thermal parameters, a reduction of the thermal motion by lowering the

Table 2. Atomic Parameters for BSP at 108 K

	x	y	z	B_{eq}/Å^2
		(×10^4)		
O	7922(1)	−2627(4)	1390(2)	1.5
N	8634(1)	−5698(4)	95(2)	0.9
C1	7338(2)	−2138(5)	−753(2)	0.9
C2	7293(2)	−1408(5)	355(2)	1.1
C3	6591(2)	652(5)	398(2)	1.4
C4	5948(2)	1950(5)	−645(2)	1.4
C5	5995(2)	1298(5)	−1753(2)	1.3
C6	6687(2)	−746(5)	−1797(2)	1.1
C7	8037(2)	−4308(5)	−845(2)	1.0
C8	9307(2)	−7841(5)	−4(2)	0.9
C9	9962(2)	−9076(5)	1072(2)	1.0
C10	10648(2)	−11206(5)	1083(2)	1.0
	x	y	z	B/Å^2
		(×10^3)		
H3	658(2)	101(6)	118(2)	2.0(0.6)
H4	543(2)	320(7)	−63(2)	2.2(0.6)
H5	553(2)	213(6)	−249(2)	1.5(0.6)
H6	673(2)	−127(6)	−259(2)	1.5(0.6)
H7	802(2)	−456(6)	−166(2)	1.7(0.6)
H9	995(2)	−841(6)	184(2)	1.4(0.6)
H10	1112(2)	−1181(6)	184(2)	0.9(0.5)
H11	837(3)	−357(9)	122(3)	7.0(1.1)

temperature was observed in all atoms except for the hydroxyl hydrogen H11. The interatomic distances and bond angles are listed in Table 3 for 108 K and room temperature. At room temperature, an alternation of bond lengths, which is expected when there exists a resonance contribution from the *o*-quinonoid structure, was recognized.[2] This tendency is less pronounced at 108 K. However, an alternation of the bond lengths still remains. From optical measurements, the energy difference between the enol and keto species was evaluated as being ca. 0.1 eV.[2] The thermal energy at 108 K is, thus, low enough to settle more than 99.99% of the molecules into the enol from. Therefore, the partial keto-like contribution seems to already exist in BSP before the color change becomes noticeable. This may be a common feature of thermochromic *N*-salicylideneanilines, since a similar partial contribution from the keto-like structure was observed in *N*-(5-chlorosalicylidene)aniline at 90 K.[4] The largest change in the bond length as a result of temperature appears in the N–C8 bond. The distance is shorter by 0.026 Å at 108 K than at room temperature. The conjugation system is not completely continuous in the limited structure of the proton-transferred species. Thus, the shorter N–C8 distance may indicate that the conjugation system is more extended at low temperatures.

Table 3. Interatomic Diastances and Bond Lengths of BSP

	Room temperature	108 K
Distance	*l*/Å	*l*/Å
C1–C2	1.404(3)	1.406(4)
C2–O	1.349(2)	1.350(3)
C2–C3	1.396(3)	1.405(4)
C3–C4	1.376(3)	1.378(3)
C4–C5	1.386(4)	1.399(4)
C5–C6	1.379(3)	1.390(4)
C1–C6	1.401(2)	1.402(3)
C1–C7	1.448(3)	1.456(4)
C7–N	1.284(2)	1.297(3)
N–C8	1.448(3)	1.422(3)
C8–C9	1.391(2)	1.398(3)
C9–C10	1.382(3)	1.391(4)
C8–C10′	1.395(3)	1.401(4)
O···N	2.607(2)	2.599(3)
Angle	*θ*/°	*θ*/°
C2–C1–C7	121.9(2)	121.8(2)
C6–C1–C2	118.5(2)	119.0(2)
C1–C2–O	121.2(2)	121.3(2)
C1–C2–C3	119.8(2)	119.8(2)
C2–C3–C4	120.1(2)	120.0(3)
C3–C4–C5	121.0(2)	121.0(3)
C4–C5–C6	119.2(2)	119.0(2)
C5–C6–C1	121.4(2)	121.1(3)
C6–C1–C7	119.6(2)	119.2(2)
C1–C7–N	121.9(2)	121.1(2)
C7–N–C8	121.6(2)	120.8(2)
N–C8–C9	116.8(2)	116.3(2)
C8–C9–C10	121.5(2)	121.3(3)
C9–C8–C10′	118.2(2)	118.6(2)
N–C8–C10′	125.0(2)	125.1(2)
C8′–C10–C9	120.4(2)	121.3(2)

The molecular packing in the lattice is practically the same as that observed at room temperature.[2] The temperature dependence of the lattice parameters are shown in Fig. 2(a). The thermal contraction is most noticeable in the *c** direction, which corresponds to the direction of side-by-side molecular arrangement. The interplanar distance between the mean molecular planes becomes shorter at 108 K (3.26 Å) than at room temperature (3.29 Å). The molecular overlap is shown in Fig. 3. This overlapping mode is convenient for the charge-transfer interaction to operate between the molecules. The azomethine (–CH=N–) groups act as an acceptor relative to the benzene rings in the OH species, and all –CH=N– groups effectively overlap with the benzene rings. When the temperature is

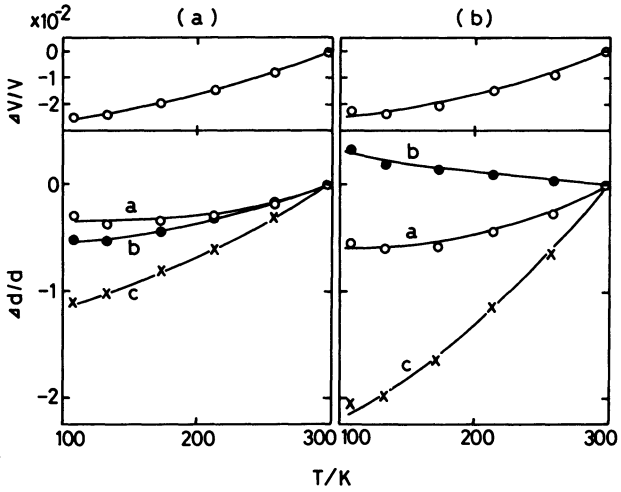

Fig. 2. Temperature dependence of lattice parameters (d and V are the room temperature parameters and volume, respectively, $\Delta d=d(T)-d$, and $\Delta V=V(T)-V$); BSP (a) and DSPY (b).

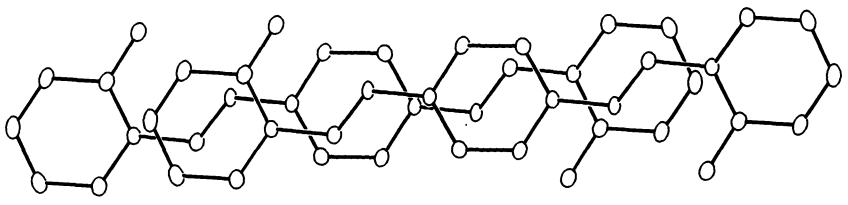

Fig. 3. Molecular overlapping between the BSP molecules.

increased, namely the content of the NH species is increased, the newly formed *p*-phenylenediamine moiety becomes a donor part and the *o*-quinonoid moiety becomes an acceptor part. The thermochromic band is, thus, assigned to the charge-transfer transition between these donor and acceptor portions.[2] Intermolecular charge-transfer interactions between such donor and acceptor portions may operate at higher temperatures.

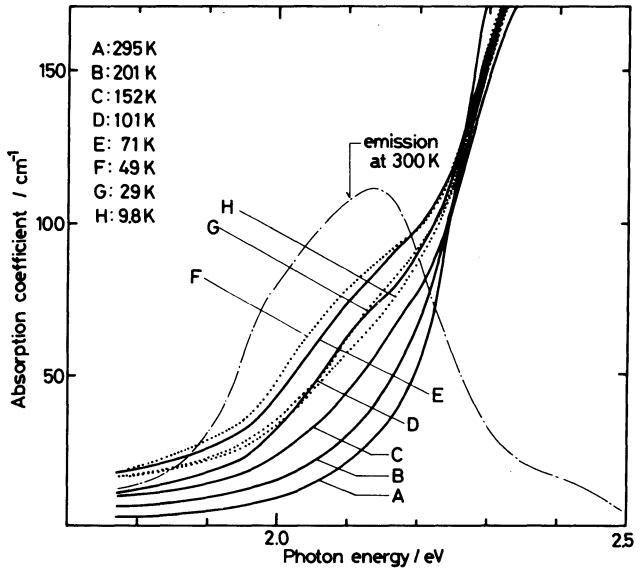

Fig. 4. Single crystal absorption spectral changes with temperature for DSPY.

DSPY. Although the molecule has a common framework with BSP, the optical properties observed for DSPY are significantly different from those observed for BSP. Figure 4 shows the single-crystal visible absorption spectra over a wide temperature range. The spectra change slightly at low temperatures. However, when the temperature is increased, noticeable growth of a new absorption observed in BSP does not occur in DSPY. The emission spectrum obtained at 300 K are also shown in Fig. 4, which corresponds well to the absorption spectra. In BSP the emission spectra show a large Stokes shift, which is a characteristic of the proton-transfer reaction. Judging from the absorption spectra, it can be concluded that the thermal proton-transfer reaction does not occur in the DSPY system.

The existence of a weak absorption band in the lower-energy region at low temperatures is interesting from a different point of view. Since this band diminishes at higher temperatures, it is obviously not related to the thermal proton transfer. In general, such growth of absorption at the lower-energy side by lowering the temperature is unusual, and the origin and mechanism of this growth in DSPY are unknown at the present stage.

The infrared spectra of DSPY were recorded at room temperature and at 6.3 K (Fig. 5). The position of the OH stretching mode shifts slightly with temperature; ca. 2800 cm^{-1} at 6.3 K, ca. 2850 cm^{-1} at room temperature. However, the peak profile does not change essentially. Thus, the results of the infrared spectra also suggests that the thermal proton-transfer process

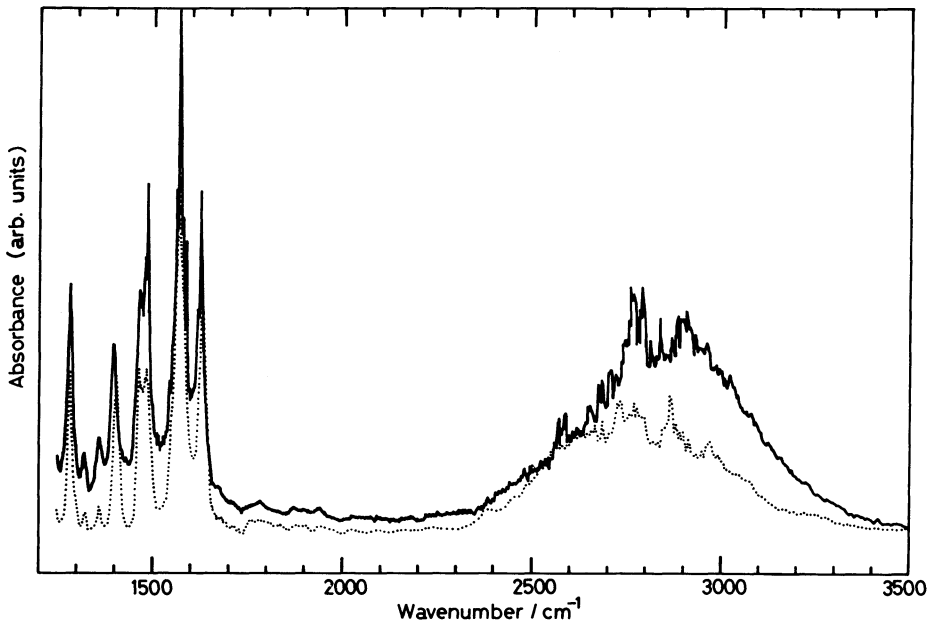

Fig. 5. Single crystal infrared spectra for DSPY at room temperature (solid line) and at 6.3 K (dotted line). The full scale does not coincide with each other because of the difference in the experimental conditions.

is absent in the DSPY system.

As shown in Fig. 6, a significant difference of the molecular structure was found by X-ray analysis. The

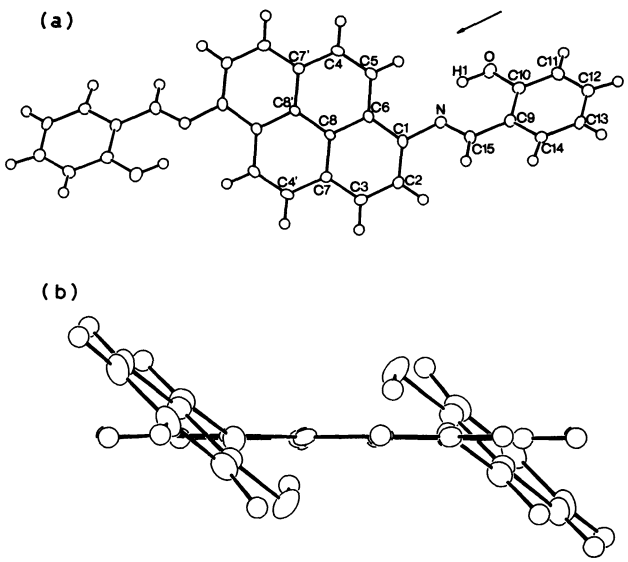

Fig. 6. ORTEP drawing of DSPY at 108 K showing the atom numbering scheme (a) and side view along the arrow indicated (b).

atomic parameters are listed in Table 4;[7] the bond lengths and angles for both temperatures are listed in Table 5. Two terminal benzene rings are tilted with respect to the central pyrene plane, and the molecule is largely deformed from the planar structure. This tilting angle does not change with temperature: 42.0° at room temperature and 42.4° at 108 K, and no significant changes of the molecular dimensions by temperature have been observed. In DSPY there is no contribution from the quinonoid structure.

The observed O···N distance is slightly longer than that of BSP. However, the difference is small and it is not likely that the difference in the optical properties arises from it. The observed frequency of the OH stretching mode of DSPY is in good agreement with the value predicted from the Novak's relationship between the position of ν_{OH} and the O···N distance.[8]

The temperature dependence of the lattice parameters are shown in Fig. 2(b), and the crystal structure at 108 K is shown in Fig. 7. By lowering temperature, the length of the *b*-axis is slightly increased, while that of the *c*-axis is decreased. Consequently, the interplanar distance between the pyrene rings is shortened, i.e., 3.43 Å at room temperature and 3.39 Å at 108 K. However, all interatomic distances between the mole-

Table 4. Atomic Parameters for DSPY

	<108 K>					<300 K>			
	x	*y*	*z*	B_{eq}/Å^2		*x*	*y*	*z*	B_{eq}/Å^2
		(×10^4)					(×10^4)		
O	6262(2)	2575(1)	7075(6)	1.8	O	6289(2)	2568(1)	7003(8)	5.3
N	4791(2)	1875(1)	3902(7)	1.3	N	4811(2)	1870(1)	3900(8)	3.5
C1	4381(2)	1276(1)	2973(8)	1.1	C1	4402(3)	1271(2)	2983(10)	3.1
C2	3362(2)	1103(1)	3603(8)	1.1	C2	3393(3)	1097(2)	3605(10)	3.4
C3	3000(2)	504(1)	2823(8)	1.2	C3	3031(3)	501(2)	2834(10)	3.2
C4	6724(2)	568(1)	−580(8)	1.1	C4	6712(3)	567(2)	−576(10)	3.3
C5	6101(3)	996(1)	821(8)	1.1	C5	6102(3)	990(2)	839(10)	3.2
C6	5051(2)	839(1)	1554(8)	0.9	C6	5060(3)	836(2)	1550(10)	2.8
C7	3631(2)	56(1)	1384(8)	1.0	C7	3648(3)	55(2)	1377(10)	2.9
C8	4671(2)	226(1)	735(8)	0.9	C8	4677(3)	225(2)	733(10)	2.7
C9	4578(3)	2973(1)	4671(8)	1.2	C9	4610(3)	2969(2)	4740(11)	3.6
C10	5588(3)	3062(2)	6455(8)	1.3	C10	5618(3)	3056(2)	6500(11)	3.9
C11	5911(3)	3656(2)	7635(9)	1.6	C11	5939(3)	3644(2)	7635(11)	4.5
C12	5242(3)	4164(2)	6998(9)	1.7	C12	5270(4)	4151(2)	7109(12)	4.9
C13	4246(3)	4088(1)	5211(9)	1.6	C13	4280(3)	4080(2)	5384(13)	4.9
C14	3924(3)	3498(1)	4071(9)	1.4	C14	3954(3)	3491(2)	4258(12)	4.5
C15	4204(3)	2361(1)	3479(8)	1.3	C15	4235(3)	2361(2)	3569(10)	3.6
	x	*y*	*z*	*B*/Å^2		*x*	*y*	*z*	*B*/Å^2
		(×10^3)					(×10^3)		
H1	595(4)	219(2)	570(15)	10.5(1.7)	H1	604(5)	218(3)	557(16)	14.8(2.0)
H2	290(2)	141(1)	474(8)	1.1(0.7)	H2	294(3)	142(2)	459(9)	5.4(1.0)
H3	226(2)	40(1)	334(8)	1.7(0.7)	H3	228(3)	34(2)	330(9)	4.7(0.9)
H4	746(3)	69(1)	−106(9)	2.0(0.9)	H4	744(3)	72(1)	−114(9)	4.5(0.9)
H5	636(2)	143(1)	136(9)	2.0(0.8)	H5	633(3)	143(2)	123(9)	5.2(1.0)
H11	660(3)	369(2)	910(12)	4.6(1.2)	H11	664(4)	371(2)	912(12)	9.1(1.4)
H12	547(4)	459(2)	827(14)	6.0(1.5)	H12	550(4)	454(2)	826(12)	8.6(1.4)
H13	377(3)	445(2)	474(10)	2.7(0.9)	H13	376(3)	448(2)	527(10)	6.0(1.0)
H14	320(3)	340(2)	276(10)	3.2(0.9)	H14	322(4)	341(2)	359(14)	11.3(1.6)
H15	345(3)	233(2)	214(9)	2.3(0.8)	H15	350(3)	231(1)	233(9)	4.3(0.9)

Table 5. Interatomic Distances and Bond Angles of DSPY

	Room temperature	108 K		Room temperature	108 K
Distance	l/Å	l/Å	N-C1-C2	121.8(3)	121.8(3)
C1-C2	1.398(6)	1.403(5)	C1-C2-C3	120.6(4)	120.4(3)
C1-C6	1.409(5)	1.412(4)	C2-C3-C7	121.5(4)	121.5(3)
C1-N	1.413(5)	1.417(4)	C5-C4-C7′	121.3(4)	121.6(3)
C2-C3	1.376(5)	1.386(4)	C4-C5-C6	121.3(3)	121.0(3)
C3-C7	1.395(5)	1.399(5)	C1-C6-C5	122.5(3)	122.3(3)
C4-C5	1.349(6)	1.358(5)	C1-C6-C8	118.9(3)	119.1(3)
C4-C7′	1.430(5)	1.435(4)	C5-C6-C8	118.6(3)	118.7(3)
C5-C6	1.437(5)	1.442(5)	C3-C7-C4′	122.4(4)	122.4(3)
C6-C8	1.418(5)	1.423(4)	C3-C7-C8	118.5(3)	118.6(3)
C7-C8	1.423(5)	1.427(4)	C4′-C7-C8	119.1(3)	119.0(3)
C8-C8′	1.426(5)	1.433(4)	C6-C8-C7	120.3(3)	120.2(3)
C9-C10	1.419(6)	1.417(5)	C6-C8-C8′	120.2(3)	120.4(3)
C9-C14	1.400(5)	1.406(5)	C7-C8-C8′	119.5(3)	119.7(3)
C9-C15	1.442(6)	1.452(5)	C10-C9-C14	118.2(4)	118.3(3)
C10-C11	1.380(6)	1.396(5)	C10-C9-C15	122.0(4)	122.0(3)
C10-O	1.356(5)	1.361(4)	C14-C9-C15	119.7(4)	119.7(3)
C11-C12	1.385(6)	1.393(5)	C9-C10-O	120.7(4)	121.2(3)
C12-C13	1.388(6)	1.398(5)	C9-C10-C11	120.2(4)	120.3(3)
C13-C14	1.381(6)	1.386(5)	O-C10-C11	119.0(4)	118.5(3)
C15-N	1.283(5)	1.285(4)	C10-C11-C12	120.0(4)	119.7(3)
O···N	2.614(4)	2.612(3)	C11-C12-C13	121.1(4)	120.9(3)
			C12-C13-C14	119.1(4)	119.2(3)
Angle	γ/°	γ/°	C9-C14-C13	121.4(4)	121.5(3)
C2-C1-C6	120.1(3)	120.1(3)	C9-C15-N	122.0(4)	121.3(3)
N-C1-C6	118.0(3)	118.0(3)	C1-N-C15	120.9(3)	120.1(3)

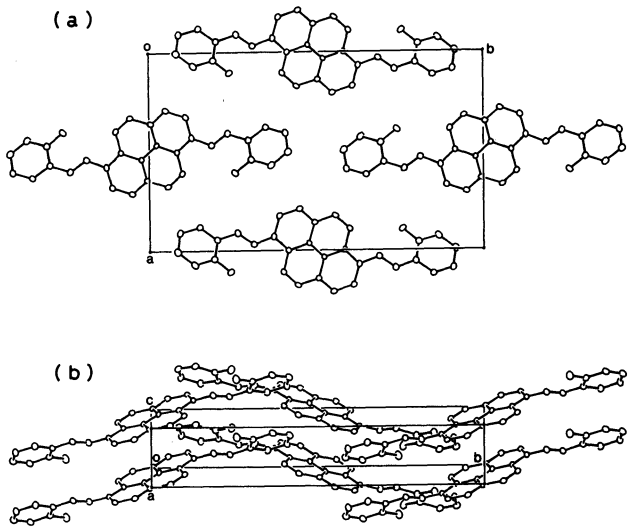

Fig. 7. Crystal structure of DSPY at 108 K; projection onto the (001) plane (a) and stacking structure (b).

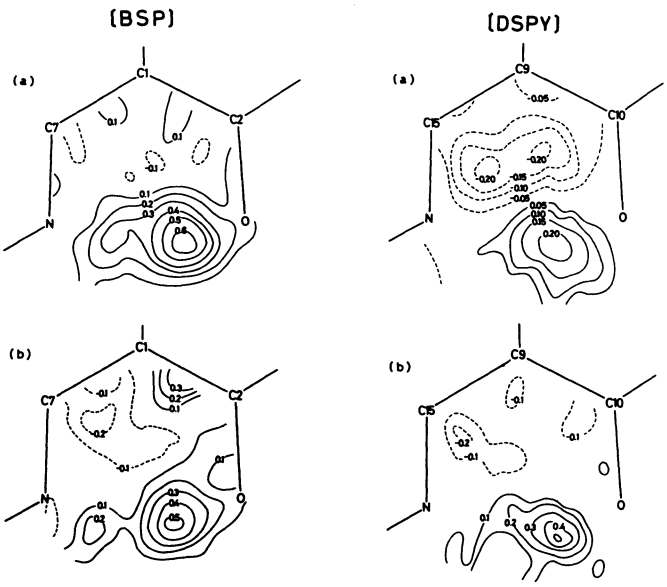

Fig. 8. Difference syntheses of the hydrogen bonded chelate ring of BSP and DSPY (e Å^{-3}); room temperature (a) and 108 K (b).

cules are larger than 3.4 Å, and there is no effective intermolecular interactions.

The results of the optical and structural studies of DSPY and BSP provide important information about the mechanism of the thermal proton transfer in *N*-salicylideneanilines. The geometrical circumstances of the hydroxyl hydrogen in DSPY are the same that in BSP. However, all data indicate no occurrence of thermal proton transfer in DSPY. In the case of BSP, the conjugation system is extended in the whole molecule, since the molecule is planar. Thus, the conjugation system in the central aromatic ring can participate in the stabilization of the partial contribution from the keto-like π-electron distribution. On the other hand, DSPY is not planar; thus, the conjugation system of the central aromatic ring is isolated from the terminal ones. In such a structure, the conjugation

system of the central aromatic group is not able to participate in the stabilization of the keto-like contribution. This seems to be important, since the partial contribution from the keto-like π-electron distribution in BSP is recognized even before the color change has become noticeable. It can therefore be concluded that one of the conditions required for the thermal proton transfer in *N*-salicylideneanilines is that the molecule is planar so that the conjugation system is sufficiently extended to be capable of the corresponding π-electron configuration of the isomer.

Another interesting feature observed in both BSP and DSPY is the large thermal parameters of the hydroxyl hydrogens, even at 108 K. Then, the difference syntheses were calculated by taking the parameters of the hydroxyl hydrogen out of the refined structures; the maps with regard to the hydrogen-bonded chelate rings are shown in Fig. 8. In DSPY, it is clearly seen that there exists only the OH proton at both temperatures. On the other hand, in addition to the OH proton, a contribution from the NH proton in BSP can be seen from the map. Thus, the differences in the optical properties between BSP and DSPY seem to be reflected in these maps. At low temperature, there still remains the contribution from the NH proton in BSP. In general, it is difficult to discuss quantitatively such a hydrogen distribution merely from the X-ray results. The microscopic aspect of the proton behavior in BSP will be clarified by more suitable techniques such as neutron diffractions or nuclear magnetic resonances.

We are grateful to Dr. Koshiro Toriumi of IMS for his helpful discussions about X-ray analysis.

References

1) The abbreviation is adopted from *N,N'*-bis(salicylidene)-*p*-phenylenediamine in Ref. 2.

2) N. Hoshino, T. Inabe, T. Mitani, and Y. Maruyama, *Bull. Chem. Soc. Jpn.*, **61**, 4207 (1988).

3) M. D. Cohen, G. M. J. Schmidt, and S. Flavian, *J. Chem. Soc.*, **1964**, 2041. E. Hadjoudis, *J. Photochem.*, **17**, 355 (1981).

4) J. Bregman, L. Leiserowitz, and G. M. Schmidt, *J. Chem. Soc.*, **1964**, 2068.

5) H. Vollman, H. Becker, M. Corell, H. Streek, and G. Langbein, *Justus Liebigs Ann. Chem.*, **531**, 1 (1937).

6) T. Sakurai and K. Kobayashi, *Rep. Inst. Phys. Chem. Res.*, **55**, 69 (1979).

7) The lists of structure factors and anisotropic thermal parameters for nonhydrogen atoms are deposited at the Office of the Editor of Bull. Chem. Soc. Jpn. (Document No. 8886).

8) A. Novak, *Struct. Bonding*, **18**, 177 (1974).

9) C. K. Johnson, ORTEP, Report ORNL-3794, Oak Ridge National Laboratory, Tennessee (1976).